Instruments and Methods

Techniques for measuring high-resolution firn density profiles: case study from Kongsvegen, Svalbard

Robert L. HAWLEY,[1] Ola BRANDT,[2] Elizabeth M. MORRIS,[1] Jack KOHLER,[2]
Andrew P. SHEPHERD,[3] Duncan J. WINGHAM[4]

[1] Scott Polar Research Institute, University of Cambridge, Lensfield Road, Cambridge CB2 1ER, UK
E-mail: rlh45@cam.ac.uk
[2] Norwegian Polar Institute, Polar Environmental Centre, NO-9296 Tromsø, Norway
[3] Department of Geography, University of Edinburgh, Drummond Street, Edinburgh EH8 9XP, UK
[4] Centre for Polar Observation and Modelling, University College London, Gower Street, London WC1E 6BT, UK

ABSTRACT. On an 11 m firn/ice core from Kongsvegen, Svalbard, we have used dielectric profiling (DEP) to measure electrical properties, and digital photography to measure a core optical stratigraphy (COS) profile. We also used a neutron-scattering probe (NP) to measure a density profile in the borehole from which the core was extracted. The NP- and DEP-derived density profiles were similar, showing large-scale (>30 cm) variation in the gravimetric densities of each core section. Fine-scale features (<10 cm) are well characterized by the COS record and are seen at a slightly lower resolution in both the DEP and NP records, which show increasing smoothing. A combination of the density accuracy of NP and the spatial resolution of COS provides a useful method of evaluating the shallow-density profile of a glacier, improving paleoclimate interpretation, mass-balance measurement and interpretation of radar returns.

1. INTRODUCTION

The snow densification process is of fundamental importance in many aspects of glaciology, including regional climatology, watershed runoff forecasting and interpretation of ice-surface elevation changes. In particular, high-resolution density profiles are critical for accurate modelling and interpretation of ground-penetrating radar (GPR) returns. In climatology studies, the thickness and frequency of refrozen melt layers are used to infer summer climate conditions (Okuyama and others, 2003), highlighting the importance of detecting thin ice layers in a density profile. In addition, the slowly varying depth–density relationship is indicative of long-term climate (e.g. Herron and Langway, 1980), and highly accurate density data are needed to exploit this for paleoclimate interpretation.

In the traditional gravimetric method, the mass and volume of a sample are measured, with resolution and accuracy being dependent upon the sample size. Such samples are generally obtained in three ways: direct sampling from a snow-pit wall; bulk sampling of core sections; and subsamples cut from core sections. The practical depth limit for snow-pit sampling is a few metres in most locations. For core sampling, bulk densities of whole sections of core will not necessarily reveal fine density stratigraphy or ice layers (as thin as ~1 mm) that would have an effect on GPR signals (Kohler and others, 1997; Arcone and others, 2004). Making smaller subsamples from the core gives finer resolution, but is time-consuming and thus rarely carried out (Clark and others, 2007) over the full length of a core. Such sampling does not coexist easily with chemistry studies on a core, so non-destructive methods are clearly beneficial.

Alternative methods for measuring the fine-scale density and stratigraphy in the firn are therefore desirable. Wilhelms (2005) expanded on the work of Wilhelms and others (1998) and Wolff (2000) using di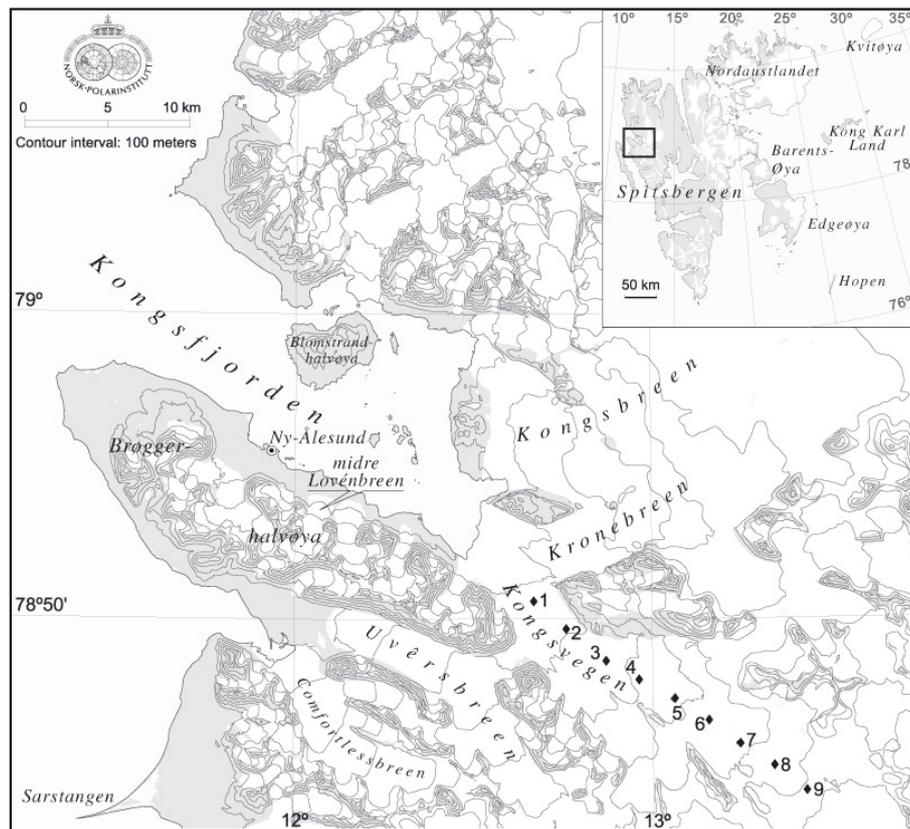electric profiling (DEP) to infer firn density from conductivity and permittivity measurements. Morris and Cooper (2003) described the adaptation of a soil moisture instrument, the neutron-scattering probe (NP), to measure snow and firn density in a borehole. The utility of this method for interpreting firn stratigraphy has been shown (Hawley and Morris, 2006; Hawley and others, 2006), and Morris (in press) presented a physically based scattering model for calibration. Hawley and Morris (2006) demonstrated a link between firn density and optical properties using borehole optical stratigraphy (BOS), and many ice-core processing lines currently use digital photography or scanning to image core sections (McGwire and others, 2007), yielding data from which to produce a similar core optical statigraphy (COS) record. Gamma-attenuation profiling, in which density can be inferred from the absorption and scattering of γ-rays by ice, has also been used (Eisen and others, 2006) to measure density non-destructively on core sections.

We use detailed measurements of density acquired by DEP and NP methods, along with traditional gravimetric measurements and COS, to assess the utility of each technique for determining detailed firn density profiles for a complex stratigraphy with snow, firn and ice layers.

2. METHODS
2.1. Study area

Kongsvegen is a 25 km long polythermal, surge glacier in Svalbard, which has been the subject of extensive mass-balance campaigns (e.g. Hagen and others, 1999). Our study site is located at mass-balance stake 8 on the glacier, at an elevation of ~700 m (Fig. 1). Melting or rain events can occur year-round in Svalbard, and air temperatures during summer remain above freezing (Førland and Hanssen-Bauer, 2000). Meltwater can therefore percolate deep into the firn, forming ice layers up to several tens of centimetres thick.

Fig. 1. Map of the Ny-Ålesund region, with the glacier Kongsvegen in the lower right. Our study site is located at stake 8.

2.2. Drilling

At our field site, we collected a firn core to a depth of ~11 m using a Polar Ice Coring Office (PICO) 10 cm hand auger with a power head. We measured and weighed the 35 core sections in the field to obtain gravimetric densities. Core quality was consistently poor in the unconsolidated winter snow comprising the uppermost 2.8 m, making it impractical to return these sections to the laboratory. We transported the remaining 23 core sections (listed in Table 1) to the laboratory for repeat gravimetric measurements, DEP and COS analysis. For registration with borehole measurements, each core section was located in depth with respect to its neighbours and several control points, at which we had measured the depth of the drill cutting head.

2.3. Neutron-probe logging

Once the drilling was complete, we lowered the neutron probe to the bottom of the borehole and raised it slowly to the surface at approximately 7–10 cm min^{-1}, with the probe offset and resting against the side of the hole, logging the density at 1 cm intervals (Morris and Cooper, 2003; Hawley and Morris, 2006). The calibration of the NP measurement depends on the exact diameter of the borehole, which is larger near the surface due to the repeated passage of the drill. The NP-measured density profile shown in Figure 2 was determined from the measured count rate of neutrons returning to the detector using three-group neutron-scattering theory (Morris, in press). The count rate depends on the characteristics of the probe, the snow/firn/ice density, temperature and the diameter of the borehole.

The diameter of most boreholes drilled in firn with a hand-held coring drill is likely to vary; the hole will be larger near

the surface from the repeated removal and insertion of the drill. We know that, in this case, the diameter of the borehole was not constant. Specifically, the topmost ~2 m of the hole were enlarged as a result of repeated raising and lowering of the drill. This effect is likely to be largest in the upper few metres and smallest at the bottom, which has seen the fewest passes of the drill. In the absence of a caliper log of the hole, we estimated the borehole diameter to be 11 cm (0.5 cm on each side of the drill head) throughout most of its depth, flaring to 14 cm at the surface (estimated visually).

As can be seen from the comparison between gravimetric and NP data in Figure 2, there is good agreement between the bulk gravimetric densities and those measured by NP. The log stops before the bottom of the core because the bottom of the hole was filled with ice chips that could not be removed by the drill.

2.4. Dielectric profiling

We measured conductivity and permittivity profiles in the laboratory using DEP at 250 KHz. We made measurements along the core sections at 5 mm increments with 10 mm electrodes. For each core section, we made four measurements, rotating the core by 0, 90, 180 and 270°. DEP measures the conductance and capacitance of the ice core, and we use the capacitance C_p, following Kohler and others (2003), to estimate the relative permittivity ϵ_r:

$$\epsilon_r = \frac{C_p}{C_{air}}, \qquad (1)$$

where $C_{air} = 64.5 \times 10^{-15}$ F m^{-1} is a constant obtained using a blank reading with an empty instrumental set-up. See Wilhelms and others (1998) for a more thorough description of

Table 1. Laboratory measurements of the core sections

Piece	Length	Diameter	Mass	Density
	m	m	kg	kg m^{-3}
1	0.290	0.0750	0.568	444 ± 10
2	0.255	0.0740	0.527	481 ± 12
3	0.285	0.0760	0.761	589 ± 13
4	0.460	0.0760	0.153	733 ± 13
5	0.400	0.0750	0.961	544 ± 10
6	0.500	0.0750	1.191	539 ± 9
7	0.370	0.0750	0.994	608 ± 12
8	0.540	0.0760	2.074	847 ± 14
9	0.570	0.0760	1.391	538 ± 9
10	0.720	0.0755	1.976	613 ± 9
11	0.465	0.0760	1.505	714 ± 12
12	0.335	0.0760	0.929	612 ± 12
13	0.330	0.0770	1.256	818 ± 16
14	0.205	0.0770	0.816	855 ± 24
15	0.155	0.0770	0.593	822 ± 29
16	0.440	0.0755	1.306	663 ± 12
17	0.090	0.0770	0.241	575 ± 33
18	0.625	0.0760	1.706	602 ± 9
19	0.290	0.0760	0.872	663 ± 14
20	0.095	0.0770	0.264	597 ± 33
21	0.110	0.0760	0.329	660 ± 31
22	0.550	0.0760	1.950	782 ± 13
23	0.130	0.0770	0.402	664 ± 27

Fig. 2. Density data (black) and data averaged over core sections (grey) to facilitate comparison: (a) gravimetric density data; (b) NP data; (c) DEP data (thin grey lines depict four runs at 0, 90, 180 and 270° rotation, and the black line depicts the mean); and (d) imagery of the core on a black background with side illumination, the basis of the COS shown in Figure 3.

the instrument and discussion of the technique. We then use the relationship between density ρ and relative permittivity ϵ_r given by Kovacs and others (1995),
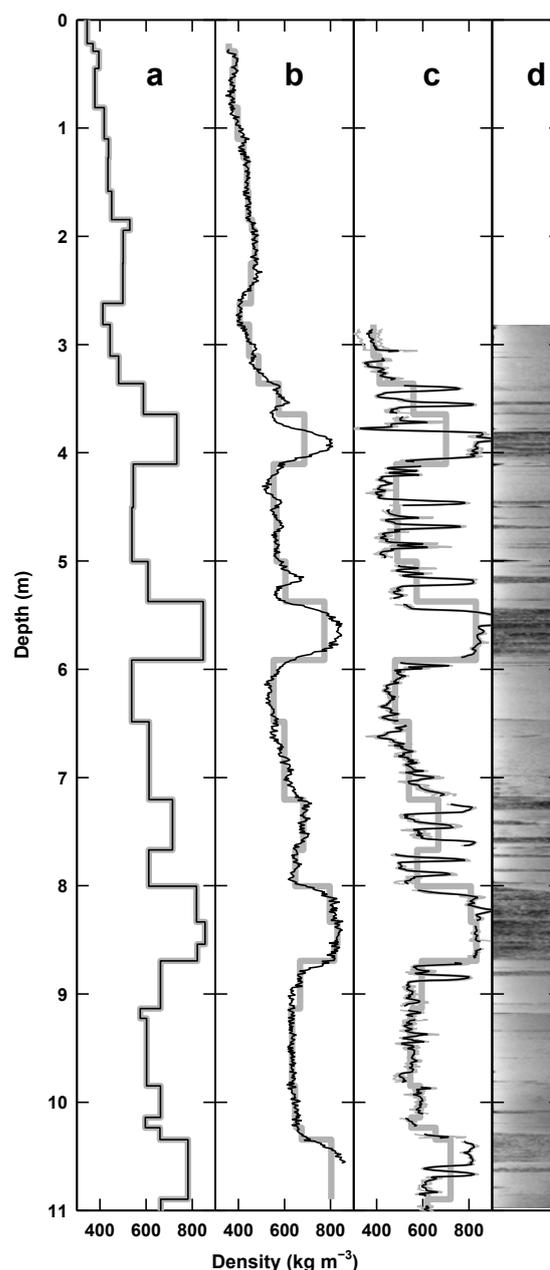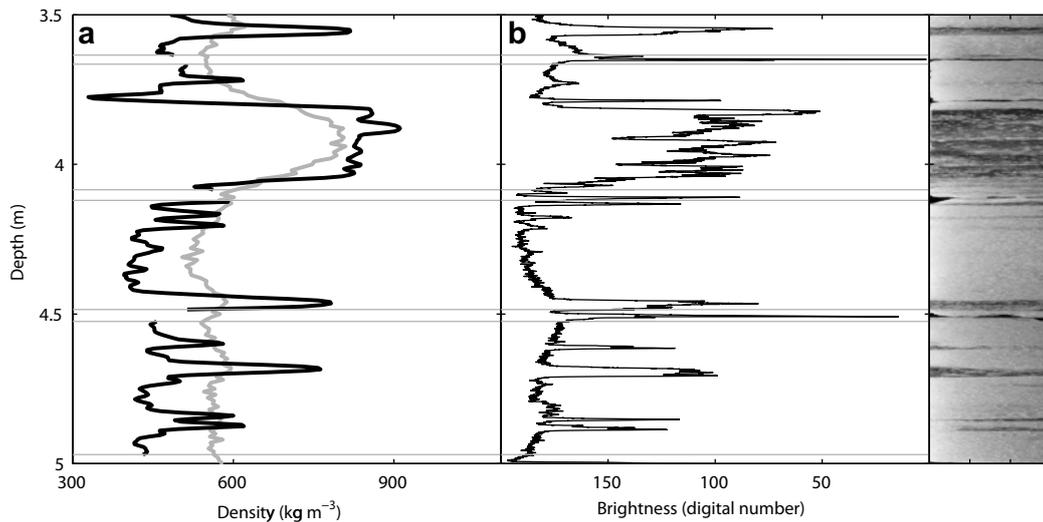
$$\epsilon_r = (1 + 8.45 \times 10^{-4}\rho)^2, \qquad (2)$$

to calculate the firn/ice density. Since DEP measures over a finite volume, the measurements near the ends of each core section are subject to end effects. We excised these low-density end-effect anomalies by eye. The full set of DEP profiles is shown in Figure 2. Note that the DEP-derived density profile appears to capture a significant amount of high-frequency variability, agrees well with gravimetric densities in high-density areas and slightly underestimates the density of the lower-density layers.

2.5. Core optical stratigraphy

Visible stratigraphy analysis on ice cores has a long history of success (e.g. Alley, 1988; Alley and others, 1997). More recently, Hawley and others (2003) have developed BOS, which takes the visual analysis concept to boreholes and measures a log of brightness vs depth. To create a COS profile, we imaged the core sections illuminated from the side with a digital camera. The details of the camera system are presented by Sjögren and others (2007).

We processed the images to obtain a brightness log by subsampling the centre portion of the image, avoiding the edges of the core, and taking the mean value of the pixels at a given depth of the core. A subsection of the optical profile with the accompanying imagery is shown in Figure 3. With side illumination, light detected by the camera is primarily scattered from within the firn, so the relatively low-scattering ice layers appear dark.

3. DISCUSSION
3.1. Accuracy of the methods

As can be seen in Figure 2, there are differences between the absolute densities measured by the three methods. We evaluate the accuracy of each technique.

The gravimetric technique using core samples has the longest history and has proven utility. The depth resolution, however, is usually insufficient to resolve the shorter-scale spatial fluctuations in density, and the accuracy can be affected by several factors. The diameter of the core is generally measured at several places along the core, but may not be consistent. The length of the core is measured, but,

Fig. 3. (a) NP (grey) and DEP (black) density profiles; (b) COS profile, a mean brightness from the core imagery; and (c) digital imagery of the core, the basis of the COS profile. In this detailed view, the effect of core breaks on the DEP and core-optical measurement can be seen; there are short data gaps where the end effects in the data have been eliminated and are delineated with horizontal grey lines. Note that thin ice layers as detected by COS are smoothed in the NP profile; this is because the 13.5 cm neutron detector behaves as a low-pass filter on the measurement. The smoothing effect is also present in the DEP profile (e.g. depths 4.4 m and 4.6 m).

in the event of an uneven core break, this length might not be uniform. This can result in density being either over- or underestimated. Often a core will be in many pieces upon extraction from the drill. If a piece is lost, the measured mass of the core section will be reduced, resulting in an underestimation of density. This is particularly troublesome when core quality is poor or in unconsolidated snow, where care is required to obtain good results. Systematic density overestimation is rare, because this would require excess weight or volume to be underestimated. Core loss also introduces an ambiguity in the depth positioning of a density measurement, although measurements of the drill depth for any given core can help to resolve this.

Density is measured by NP by counting the rate of neutrons slowed by scattering in the snow and then absorbed by the detector. The diameter of the borehole has an effect on the relation between density and count rate, as does the position of the probe in the hole, i.e. whether the probe is centred in the hole or lying against the side (Morris, in press). On Kongsvegen we did not measure borehole diameter but were careful to align the probe with the side of the hole when we set up the measurement. Although it is reasonable to assume the probe did not at any depth lose contact with the wall, we cannot categorically exclude this possibility. In future tests, use of a pressure shoe to hold the tool against the borehole wall would eliminate this source of uncertainty.

We have assumed in section 2.3 that the diameter of the hole is 11 cm through most of its depth, but that it flares from 11 cm at the first hard layer (∼2 m) to 14 cm at the surface. We do not know what the error in this estimate is, but sensitivity calculations by Morris (in press) indicate that for a 10% error in borehole diameter the resulting error in the derived density would be of the order 8–10%. A caliper log of the hole, showing the exact diameter, would allow us to account for the effect of variation in borehole diameter more accurately, although the calipers may not work properly in unconsolidated snow.

In standard practice, when co-registration of NP profiles with core is not required, the borehole can be drilled using a 5 cm non-coring auger and a rigid guide tube up to several metres long. The guide tube is made of aluminium which does not affect the neutrons, and can be left in place during logging. This prevents collapse of lower-density layers and ensures the hole is of constant diameter through the uppermost (generally lowest-density and weakest) part of the firn. In addition, the accuracy of the method is much improved by using a small-diameter access hole (Morris and Cooper, 2003; Morris, in press).

DEP uses the electrical properties of the ice, as outlined above, to calculate density. As can be seen in Figure 2, DEP appears to underestimate in the lower-density sections of core but agrees with the gravimetric measurements for the higher-density sections.

We suspect the underestimation at lower densities is caused by thinner core diameter (typically 7.3–7.6 cm compared to 7.8 cm for ice layers). The air gap between the core, guarding and electrodes in the DEP affects the capacitance readings. In essence, by reducing the core diameter by 5 mm, 13% less core material will occupy the cradle and thus the relative permittivity will be underestimated. Propagating this error through Equation (2) leads to a possible error of up to 20% in the low-density sections and 10–13% in the high-density sections. However, since the higher-density sections typically have a smaller air gap, the uncertainty is further reduced. The actual observed underestimation in the low-density parts of the core is ∼15%.

In addition, there could also be a change in conductivity with density which is unaccounted for in the density calculation, or an inaccuracy of the blank measurement. For the purposes of characterizing the large-scale fluctuations of this layered (firn/ice) core, the present method is sufficient. For a polar firn core, where density is more slowly varying, one would process the DEP using the full permittivity and conductivity values following Wilhelms (2005).

3.2. Details in the density profile

The three density measurements are plotted together in Figure 2. Both DEP and NP techniques show finer spatial resolution compared to the gravimetric method. Figure 3 shows a section of the DEP, NP and COS profiles, along with composite imagery of the core. The sharpest contrasts are seen in the COS profile. Thin ice layers such as that seen at ~4.4 m are spatially resolved by COS, and can be seen smoothed in the NP and DEP profiles. The smoothing of thin ice layers in the NP data is readily apparent. This is due to the fact that the active length of the neutron detector (13.5 cm) acts as a low-pass filter (with a cut-off of approximately half the active length, or 6.75 cm). This is particularly noticeable at ~3.75 m in Figure 3. Less obvious but also apparent is the smoothing effect of DEP with electrodes 10 mm long which sample a finite volume. A first estimate of the sensing volume can be found when excising the core-break end effects from the DEP record. Generally, ~2 cm was removed from each end of a core section, implying that the sensing length along the core is ~4 cm.

In principle, the true density profile could be extracted by inverse methods, using the NP or DEP densities and geometry constrained by COS. Since optical stratigraphy can be obtained using down-hole techniques (i.e. BOS), a combination of NP and BOS would allow a very accurate and detailed density profile to be constructed.
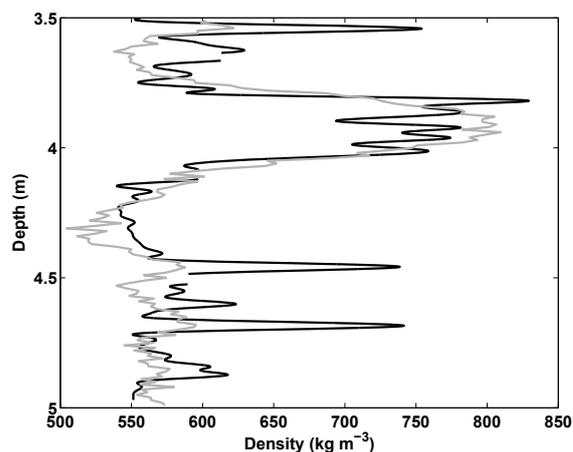
3.3. Pseudo-density from COS

Since the optical signal is affected by factors other than density, such as grain size and shape and other aspects of firn microstructure, the inversion of optical brightness to find density is not straightforward. A true inversion is beyond the scope of this study. We can, however, exploit the strong correlation between brightness and density (Hawley and Morris, 2006; Sjögren and others, 2007) to investigate the potential for an optical record (COS or BOS) to be used in combination with a high-resolution density profile (such as that from NP or DEP) to produce a detailed and accurate interpretation of density.

Simplifying the procedure of Sjögren and others (2007) for obtaining a density profile from COS, we apply a linear transformation $y = Ax + B$ to the intensity data, and vary A and B to minimize the mismatch over a short depth range between this 'pseudo-density' profile and the density profile measured by NP. The optimum values are $A = -2.4$ and $B = 1000$, and the resulting profile is shown in Figure 4. Note that the ice layers are very clearly seen in the pseudo-density profile, and the background density is in agreement with the NP density profile.

4. CONCLUSIONS

We have made side-by-side density measurements in mixed firn and ice using NP, DEP, COS and gravimetric density measurement techniques. Unconsolidated snow near the surface affects the measurements derived from all the techniques, and further refinements are needed for these conditions.

Although dependent on an accurate measurement of borehole diameter, the NP method does not require the collection and shipping of core and is relatively simple to deploy in the field. This means that the NP method is free of the problems associated with core depth registration, core breaks, poor core quality or melting of cores during shipping. In fact, NP

Fig. 4. A 'pseudo-density' profile, derived from the COS profile and a simple linear transformation, is shown in black with the NP-density data in grey. Note that while not giving a true physically based measurement of density, the COS-derived pseudo-density profile clearly captures the details of the ice layers.

can be deployed in a rapidly drilled hole with a 5 cm non-coring auger.

The DEP method has the fine resolution needed to characterize thin (<5 cm) ice layers, but suffers from the problems associated with collecting cores mentioned above. Although both NP and DEP smooth the density profile to some extent, both offer a vast improvement over gravimetric methods of density profiling, with increased spatial resolution and precision and reduced potential for human errors.

Optical stratigraphy in the borehole or on the core, while not providing a quantification of density, can be combined with either NP or DEP to improve the ability of either technique to resolve thin ice layers. A combined NP, optical and caliper down-hole tool may prove to be the ideal means of measuring a continuous, high-resolution, high-accuracy profile of density from the surface to any depth accessible via drilling.

ACKNOWLEDGEMENTS

REFERENCES

Alley, R.B. 1988. Concerning the deposition and diagenesis of strata in polar firn. *J. Glaciol.*, **34**(118), 283–290.

Alley, R.B. *and 11 others.* 1997. Visual-stratigraphic dating of the GISP2 ice core: basis, reproducibility, and application. *J. Geophys. Res.*, **102**(C12), 26,367–26,382.

Arcone, S.A., V.B. Spikes, G.S. Hamilton and P.A. Mayewski. 2004. Stratigraphic continuity in 400 MHz short-pulse radar profiles of firn in West Antarctica. *Ann. Glaciol.*, **39**, 195–200.

Clark, I.D. *and 8 others.* 2007. CO$_2$ isotopes as tracers of firn air diffusion and age in an Arctic ice cap with summer melting, Devon Island, Canada. *J. Geophys. Res.*, **112**(D1), D01301. (10.1029/2006JD007471.)

Eisen, O., F. Wilhelms, D. Steinhage and J. Schwander. 2006. Improved method to determine radio-echo sounding reflector depths from ice-core profiles of permittivity and conductivity. *J. Glaciol.*, **52**(177), 299–310.

Førland, E.J. and I. Hanssen-Bauer. 2000. Increased precipitation in the Norwegian Arctic: true or false? *Climatic Change*, **46**(4), 485–509.

Hagen, J.O., K. Melvold, T. Eiken, E. Isaksson and B. Lefauconnier. 1999. Mass balance methods on Kongsvegen, Svalbard. *Geogr. Ann.*, **81A**(4), 593–601.

Hawley, R.L. and E.M. Morris. 2006. Borehole optical stratigraphy and neutron-scattering density measurements at Summit, Greenland. *J. Glaciol.*, **52**(179), 491–496.

Hawley, R.L., E.D. Waddington, R.A. Alley and K.C. Taylor. 2003. Annual layers in polar firn detected by borehole optical stratigraphy. *Geophys. Res. Lett.*, **30**(15), 1788. (10.1029/2003GL017675.)

Hawley, R.L., E.M. Morris, R. Cullen, U. Nixdorf, A.P. Shepherd and D.J. Wingham. 2006. ASIRAS airborne radar resolves internal annual layers in the dry-snow zone of Greenland. *Geophys. Res. Lett.*, **33**(4), L04502. (10.1029/2005GL025147.)

Herron, M.M. and C.C. Langway, Jr. 1980. Firn densification: an empirical model. *J. Glaciol.*, **25**(93), 373–385.

Kohler, J., J. Moore, M. Kennett, R. Engeset and H. Elvehøy. 1997. Using ground-penetrating radar to image previous years' summer surfaces for mass-balance measurements. *Ann. Glaciol.*, **24**, 355–360.

Kohler, J., J.C. Moore and E. Isaksson. 2003. Comparison of modelled and observed responses of a glacier snowpack to ground-penetrating radar. *Ann. Glaciol.*, **37**, 293–297.

Kovacs, A., A.J. Gow and R.M. Morey. 1995. The in-situ dielectric constant of polar firn revisited. *Cold Reg. Sci. Technol.*, **23**(3), 245–256.

McGwire, K.C. *and 6 others*. In press. An integrated system for optical imaging of ice cores. *Cold Reg. Sci. Technol.*

Morris, E.M. In press. A theoretical analysis of the neutron-scattering method for measuring snow and ice density. *J. Geophys. Res.*

Morris, E.M. and J.D. Cooper. 2003. Density measurements in ice boreholes using neutron scattering. *J. Glaciol.*, **49**(167), 599–604.

Okuyama, J., H. Narita, T. Hondoh and R.M. Koerner. 2003. Physical properties of the P96 ice core from Penny Ice Cap, Baffin Island, Canada, and derived climatic records. *J. Geophys. Res.*, **108**(B2), 2090. (10.1029/2001JB001707.)

Sjögren, B. *and 6 others*. 2007. Determination of firn density in ice cores using image analysis. *J. Glaciol.*, **53**(182), 413–419.

Wilhelms, F. 2005. Explaining the dielectric properties of firn as a density-and-conductivity mixed permittivity (DECOMP). *Geophys. Res. Lett.*, **32**(16), L16501. (10.1029/2005GL022808.)

Wilhelms, F., J. Kipfstuhl, H. Miller, K. Heinloth and J. Firestone. 1998. Precise dielectric profiling of ice cores: a new device with improved guarding and its theory. *J. Glaciol.*, **44**(146), 171–174.

Wolff, E. 2000. Electrical stratigraphy of polar ice cores: principles, methods, and findings. *In* Hondoh, T., *ed. Physics of ice core records.* Sapporo, Hokkaido University Press, 155–171.